

## On the Complex Chemistry of the Uranyl Ion

### III. The Complexity of Uranyl Thiocyanate An Extinctionmetric Investigation

STEN AHRLAND

*Department of Inorganic and Physical Chemistry, Chemical Institute, University of Lund,  
Lund, Sweden*

In the preceding paper of this series (Ahrland<sup>1</sup>, in the following referred to as II) it was shown that the complexity of uranyl salts may be correctly determined extinctionmetrically as well as potentiometrically. This was very valuable as many uranyl salts cannot be investigated by anyone of the well-proved potentiometric methods which are in use (for a survey of these, see Fronaeus<sup>2</sup>). On the other hand, the salts are coloured and therefore possible to measure extinctionmetrically.

Unfortunately, the extinctionmetric method has a very serious limitation: it is impossible to use as soon as polynuclear complexes exist in the solutions. Moreover, the criterion of the existence of such complexes, stated in II, p. 803, is not very reliable. So a polynuclear complex formation may be easily overlooked and 'constants' of no physical meaning calculated. A more reliable criterion is required and the following one, pointed out by Güntelberg<sup>3, p. 76</sup> permits no doubt a surer decision between the existing possibilities.

Güntelberg recommends that measurements should be carried out at several wave-lengths. If the same result is obtained in all cases, it is reliable. The reason is very clearly seen from the formula of Fronaeus<sup>2, p. 90</sup>: while  $\beta_1$  is independent of the wave-length when the complex formation is mononuclear ( $\epsilon'_1 = 0$ ), the false 'constant' obtained in the presence of dinuclear complexes depends upon the value of the ratio  $\epsilon'_1/\epsilon_1$ ;  $\epsilon'_1$  and  $\epsilon_1$  being the molar extinctions of the first dinuclear and the first mononuclear complex respectively. The value of this ratio is likely to be changed at a sufficient great change of the wave-length and hence the 'constant' changes, too. In such a way the false 'constants' may be unveiled. One also concludes, however, that the wave-

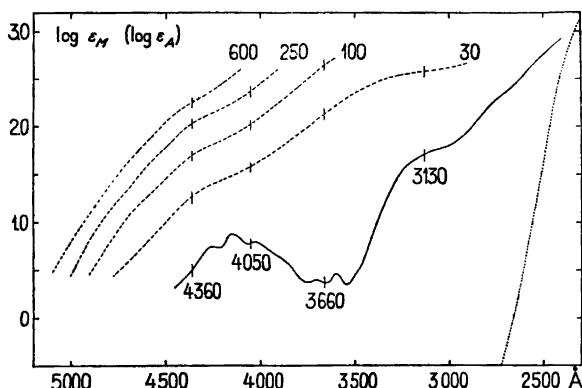


Fig. 1. Extinctions curves of a) uranyl ion (fulldrawn), b) complex solutions with  $C_M = 33.1$  mC,  $C_A = 30, 100, 250$  and  $600$  mC (dashed) and c) thiocyanate ion (dotted; the molar extinction in this case is  $\epsilon_A = \frac{E}{C_A \cdot d}$ );

lengths for measuring must be chosen in such a distance from each other that a perceptible change of the proportion between the  $\epsilon$ :s really is likely to occur. Preferably the wave-lengths should be chosen in different bands of the spectrum. In practice, however, the possibilities of a choice are, as a rule, rather restricted.

The present investigation aims to determine the complexity of the uranyl thiocyanate system merely according to the extinctions method. The apparatus and the mode of calculation used have been described in II. The calculations are, however, somewhat modified because of the particular properties of the system in question. The modifications will be closer described below.

The solutions measured all contained 100 mC  $\text{HClO}_4$ ; from the hydrolysis measurements of the first paper of this series (Ahrland<sup>4</sup>, in the following referred to as I) it can be seen that the hydrolysis of  $\text{UO}_2^{2+}$  may be completely neglected at such a high acidity. The fundamental equations (21) and (22) of II are thus valid here without the somewhat uncertain hydrolysis corrections discussed in II. p. 805. A complex formation between  $\text{H}^+$  and  $\text{SCN}^-$  is not to be feared, as thiocyanic acid belongs to the strongest acids known. This has been proved conductometrically by Ostwald<sup>5</sup> and, recently, potentiometrically by Gorman and Connell<sup>6</sup>.

As before, all solutions had the constant ionic strength  $I = 1$ .  $\text{NaClO}_4$  was used as the supplementary neutral salt. The determinations were made at  $20^\circ \text{C}$ .

Table 1. Direct determined values of  $\epsilon_M - \epsilon_0$  at given  $C_A$  and  $C_M$ .Table 1 A:  $\lambda_2 = 4360 \text{ \AA}$ .

$d \rightarrow$ cm	0.1		0.3		1		3		10	
$C_A$ mC	$C_M$ mC	$\epsilon_M - \epsilon_0$ $\text{C}^{-1} \cdot \text{cm}^{-1}$	$C_M$ mC	$\epsilon_M - \epsilon_0$ $\text{C}^{-1} \cdot \text{cm}^{-1}$	$C_M$ mC	$\epsilon_M - \epsilon_0$ $\text{C}^{-1} \cdot \text{cm}^{-1}$	$C_M$ mC	$\epsilon_M - \epsilon_0$ $\text{C}^{-1} \cdot \text{cm}^{-1}$	$C_M$ mC	$\epsilon_M - \epsilon_0$ $\text{C}^{-1} \cdot \text{cm}^{-1}$
10					104.5	3.87	28.01	5.22	7.83	5.83
20					60.2	8.98	16.73	10.75	4.90	11.53
30					39.13	14.57	11.74	16.35	3.46	16.70
50			104.4	18.63	24.95	24.92	7.78	26.85		
75			67.0	31.10	16.73	37.49	5.41	39.39		
100			50.4	42.9	13.41	48.9	4.22	50.5		
150			33.73	64.7	9.66	70.2	3.122	71.8		
200	96.0	69.5	26.78	83.7	7.65	88.4				
300	65.4	104.5	19.70	116.5	5.69	121.6				
400	50.9	135.1	15.83	145.1	4.63	149.7				

The *sodium thiocyanate puriss.* used was recrystallised from water by the same method as was mentioned for  $\text{NaClO}_4$  in I, p. 382. Dried at  $150^\circ$ . The salt was free from  $\text{Cl}^-$  when tested according to Mann<sup>7</sup>. Analysis according to Volhard gave the equivalent weight 81.3, calc. 81.1. — The other chemicals were the same as before.

To select the wave-lengths  $\lambda$  most suitable for the measurements with the accurate light-electric apparatus, extinction curves of solutions with  $C_M = 33.1$  mC and  $C_A = 30, 100, 250$  and  $600$  mC were spectrographically determined. In Fig. 1, these curves are compared with that of  $\text{UO}_2^{2+}$ , obtained from I. The positions of the strong mercury lines which serve as light sources in the light-electric apparatus are also indicated.

Table 1 B.  $\lambda_1 = 3660 \text{ \AA}$ .

$d \rightarrow$ cm	0.1		0.3		1	
$C_A$ mC	$C_M$ mC	$\epsilon_M - \epsilon_0$ $\text{C}^{-1} \cdot \text{cm}^{-1}$	$C_M$ mC	$\epsilon_M - \epsilon_0$ $\text{C}^{-1} \cdot \text{cm}^{-1}$	$C_M$ mC	$\epsilon_M - \epsilon_0$ $\text{C}^{-1} \cdot \text{cm}^{-1}$
20	95.1	70.8	24.70	93.8	6.73	102.5
30	56.4	121.4	16.08	144.7	4.57	152.0
50	32.16	220.8	9.92	242.9	2.947	249.0

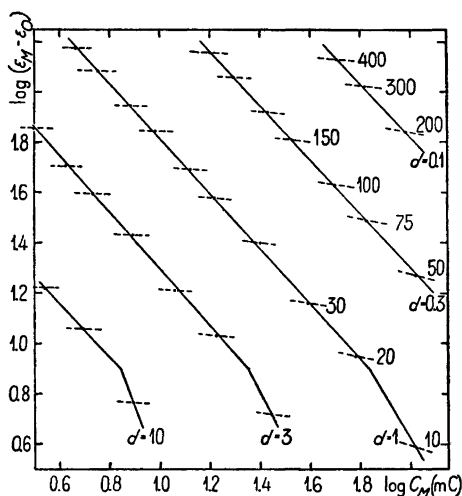


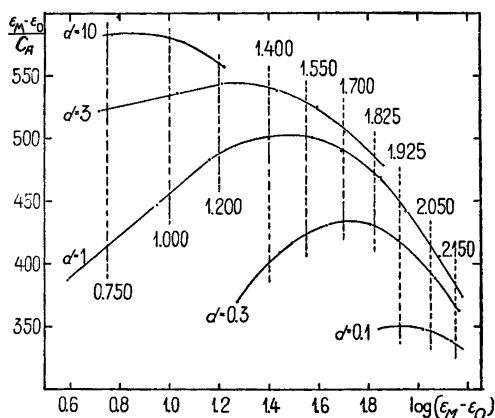
Fig. 2.  $\log(\epsilon_M - \epsilon_0)$  as a function of  $\log C_M$  at different  $d$ ;  $\lambda_2 = 4360 \text{ \AA}$ . — ●: experimentally determined points. — Full-drawn curves: the established connections between  $\epsilon_M - \epsilon_0$  and  $C_M$  for given  $d$ . — Dashed curves: position of points with constant  $C_A$ , given to the right.

It can be seen that the effect of the complex formation is especially great in the region of the mercury line  $\lambda_1 = 3660 \text{ \AA}$ . This line was thus selected for measurements, though  $\epsilon_M$  of the complex solutions are so high here that  $C_A$  cannot be increased over 50 mC in the measurements below. Still one other suitable mercury line should be selected and evidently at lower  $\epsilon_M$ , i. e. longer

Table 2.  $\epsilon_M - \epsilon_0$  at given  $C_A$ , corrected so as to fit those connections which are established between  $\epsilon_M - \epsilon_0$  and  $C_M$ .

$\lambda \rightarrow$ Å	4360					3660		
$d \rightarrow$ cm	0.1	0.3	1	3	10	0.1	0.3	1
$C_A$ mC	$\epsilon_M - \epsilon_0 \quad \text{C}^{-1} \cdot \text{cm}^{-1}$							
10			3.87	5.22	5.83			
20			8.93	10.72	11.53	71.1	93.8	102.5
30			14.52	16.33	16.70	121.1	144.7	152.0
50		18.49	25.00	26.92		220.8	242.9	249.0
75		31.12	37.58	39.36				
100		43.05	49.0	50.5				
150		64.7	70.3	71.8				
200	69.5	83.7	88.4					
300	104.5	116.5	121.6					
400	135.1	144.9	149.7					

Fig. 3.  $(\epsilon_M - \epsilon_0)/C_A$  as a function of  $\log(\epsilon_M - \epsilon_0)$  at different  $d$ ;  $\lambda_2 = 4360 \text{ \AA}$ . — The curves are cut at ten  $\log(\epsilon_M - \epsilon_0)$ , each of them representing a certain pair of  $(n, [A])$ .



wave-lengths. The line  $\lambda_2 = 4360 \text{ \AA}$  was chosen because  $\epsilon_M$  has here a suitable size so that  $C_A$  may be varied within a wide range; at the same time, the line is fairly distant from  $3660 \text{ \AA}$ .

The extinction curve of the thiocyanate ion was also determined and is given in Fig. 1. In the whole the result agrees with that obtained by v. Kiss and Csokan<sup>8</sup> for potassium thiocyanate. However, at very small  $\epsilon_A$  their curve is situated higher than the present one, undoubtedly due to traces of impurities in their salt used. One can see, that the extinction of the thiocyanate ion does not at all affect the measurements at the selected  $\lambda$ .

The thiocyanate curve is of a type characteristic of the halogenides; it rises in the ultra-violet parallel to and between the curves of bromide and iodide (about these, see Fromherz and Menschick<sup>9</sup>). Kept in a glass-stoppered bottle, the 1.00 C sodium thiocyanate solution was completely stable, as judged by the fact that quite the same extinction curve was obtained after one year of storage.

After suitable  $\lambda$  had been selected, the measurements with the light-electric apparatus were carried out. To begin with, the molar extinctions of the uranyl ion  $\epsilon_0$  were determined. At  $4360 \text{ \AA}$ , two solutions were measured:  $C_M = 72.8 \text{ mC}$  with  $d = 3 \text{ cm}$  and  $C_M = 22.14 \text{ mC}$  with  $d = 10 \text{ cm}$ .  $\epsilon_0$  was found to be 3.068 and 3.061 respectively; mean  $3.065 \text{ C}^{-1} \cdot \text{cm}^{-1}$ , a spread of  $\pm 1 \%$ . Thus Beers law is strictly valid in this case. At  $3660 \text{ \AA}$ ,  $C_M = 30.99 \text{ mC}$  was measured with  $d = 10 \text{ cm}$ . The value found was  $\epsilon_0 = 2.28 \text{ C}^{-1} \cdot \text{cm}^{-1}$ .

Then the determinations of  $\epsilon_M$  at varying  $C_A$  were performed. Here the solutions measured prove to be not at all sensitive to the day-light, what is contrary to the behaviour of chloroacetate (II, p. 804), and organic uranyl salts in general (Gmelin<sup>10</sup>). The extinctions were always reproducible within

Table 3.  $C_A$  as a function of  $C_M$  at the selected constant values of  $\log(\epsilon_M - \epsilon_0)$ .Table 3 A.  $\lambda_2 = 4360 \text{ \AA}$ .

$d \rightarrow$ cm	0.1		0.3		1		3		10	
$\log(\epsilon_M - \epsilon_0)$	$C_A$ mC	$C_M$ mC	$C_A$ mC	$C_M$ mC	$C_A$ mC	$C_M$ mC	$C_A$ mC	$C_M$ mC	$C_A$ mC	$C_M$ mC
0.750					13.58	84.9	10.73	27.1	9.65	7.9
1.000					21.93	56.2	18.69	18.7	17.21	5.6
1.200					32.55	36.6	29.14	12.3	28.30	3.7
1.400			62.6	81.3	50.2	23.9	46.4	8.1		
1.550			83.7	58.9	70.8	17.5	67.2	5.9		
1.700			115.5	42.8	102.1	12.7	98.9	4.3		
1.825			155.1	32.7	141.3	9.8	137.8	3.4		
1.925	239.7	79.8	200.8	26.5	187.0	8.0				
2.050	324	60.7	286	20.5	271	6.2				
2.150	422	48.8	386	16.7	369	5.0				

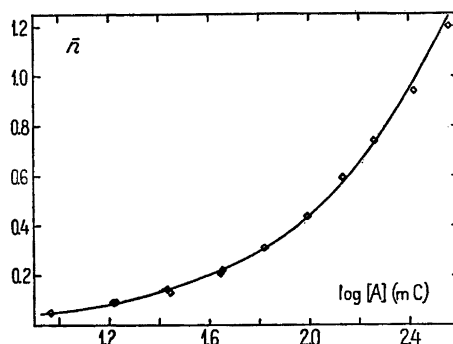
2—3‰ when a solution was prepared anew. Such a control was made for one third of the solutions.

The determined corresponding values of  $\epsilon_M - \epsilon_0$ ,  $C_A$  and  $C_M$  for  $\lambda_2$  and  $\lambda_1$  are given in Table 1 A and 1 B. In Fig. 2, the function  $\log(\epsilon_M - \epsilon_0) = f(\log C_M)$  at  $\lambda_2 = 4360 \text{ \AA}$  is given for the different values of the parameter  $d$  used. Those straight lines are drawn which represent a known connection between the quantities  $\epsilon_M - \epsilon_0$  and  $C_M$ . In the present case, three of the five lines must be broken in order to fit the lowest experimental points as well as it is required. Also for  $\lambda_1 = 3660 \text{ \AA}$ , such connections are established. From

Table 3 B.  $\lambda_1 = 3660 \text{ \AA}$ .

$d \rightarrow$ cm	0.1		0.3		1	
$\log(\epsilon_M - \epsilon_0)$	$C_A$ mC	$C_M$ mC	$C_A$ mC	$C_M$ mC	$C_A$ mC	$C_M$ mC
1.950	23.60	76.0	19.08	25.7	17.33	7.6
2.150	34.09	49.0	29.35	16.6	27.81	5.0
2.350	50.7	31.5	46.1	10.7	44.8	3.2

Fig. 4. The complex formation function. —  $\diamond$  and  $\bullet$ : values determined at  $\lambda_2 = 4360$  Å and  $\lambda_1 = 3660$  Å respectively. — The curve is obtained from the complexity constants finally calculated.



the points of intersection between those lines and the lines of constant  $C_A$  (dashed in Fig. 2) new values of  $\varepsilon_M - \varepsilon_0$  are obtained which fit the established connection between  $\varepsilon_M - \varepsilon_0$  and  $C_M$  at the  $d$  in question (Table 2). So we have now obtained  $\varepsilon_M - \varepsilon_0$  as a function of  $C_A$  at different  $d$ , with  $C_M$  known for every point.

These functions should now be cut at a number of constant  $\varepsilon_M - \varepsilon_0$  which each represents a certain constant value of  $\bar{n}$  and  $[A]$ . To perform these sections with great accuracy at a moderate size of the figure, it is in the present case convenient to transform the functions into

$$\frac{\varepsilon_M - \varepsilon_0}{C_A} = f(\log(\varepsilon_M - \varepsilon_0)) \quad (1)$$

Table 4. The corresponding values of  $[A]$ ,  $\bar{n}$  and  $\bar{n}/[A]$  obtained from the figures of Table 3.

$\lambda_2 = 4360$ Å				$\lambda_1 = 3660$ Å			
$\log(\varepsilon_M - \varepsilon_0)$	$[A]$ mC	$\bar{n}$	$\bar{n}/[A]$ C <sup>-1</sup>	$\log(\varepsilon_M - \varepsilon_0)$	$[A]$ mC	$\bar{n}$	$\bar{n}/[A]$ C <sup>-1</sup>
0.750	9.29	0.0515	5.55	1.950	16.7	0.092	5.5
1.000	16.8	0.093	5.55	2.150	27.1	0.144	5.3
1.200	27.7	0.130	4.7	2.350	44.0	0.208	4.75
1.400	44.8	0.220	4.9				
1.550	65.4	0.31	4.75				
1.700	96.8	0.435	4.5				
1.825	135.7	0.595	4.4				
1.925	181	0.74	4.1				
2.050	265	0.94	3.55				
2.150	364	1.20	3.3				

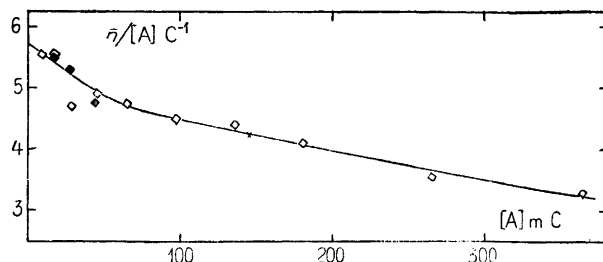


Fig. 5.  $\bar{n}/[A]$  as a function of  $[A]$ , the integration of which gives  $X([A])$  (Table 5). — The signs relate to the same measurements as in Fig. 4; but the curve is here drawn according to the experimental points.

The functions so obtained are given for  $\lambda_2 = 4360 \text{ \AA}$  in Fig. 3. They are cut at ten constant  $\log(\epsilon_M - \epsilon_0)$ , each representing a certain  $C_A$  originally used. The corresponding functions of  $\lambda_1 = 3660 \text{ \AA}$  are cut at three  $\log(\epsilon_M - \epsilon_0)$ . From the points of intersection  $C_A$  is obtained and from Fig. 2 one gets the corresponding value of  $C_M$ . The results are found in Table 3 A and 3 B. When the pairs of  $(C_A, C_M)$  so found are plotted in a diagram, straight lines are obtained within the limits of experimental error. No sign of polynuclear complex formation shows by use of this first criterion, which, however, was

Table 5.  $X([A])$ ,  $X_1([A])$  and  $X_2([A])$  for given  $[A]$ , giving the complexity constants. — The ligand number and the composition of the system as calculated from these constants.

$$\beta_1 = 5.7 \pm 0.3 \text{ C}^{-1} \quad \beta_2 = 5.5 \pm 1 \text{ C}^{-2} \quad \beta_3 = 15 \pm 5 \text{ C}^{-3}$$

[A] mC	(5a)* $\ln X([A])$	$X([A])$	(7a) $X_1([A])$ $\text{C}^{-1}$	(7b) $X_2([A])$ $\text{C}^{-2}$	(2) $\bar{n}$	(8a) $a_0$ %	(8b) $a_1$ %	(8b) $a_2$ %	(8b) $a_3$ %
10	0.0559	1.058	5.8						
20	0.1100	1.116	5.8		0.106	89.5	10.5	0	0
30	0.1624	1.176	5.9						
50	0.2629	1.301	6.0	6	0.245	77	22	1	0
75	0.3819	1.465	6.2	6.5					
100	0.4958	1.642	6.4	7	0.44	61	34.5	3.5	1
150	0.7128	2.040	6.9	8					
200	0.9175	2.503	7.5	9	0.785	40	46	9	5
250	1.1102	3.035	8.1	9.5					
350	1.4611	4.311	9.5	11	1.22	23	46.5	15.5	15

\* These figures refer to the formulas of II.



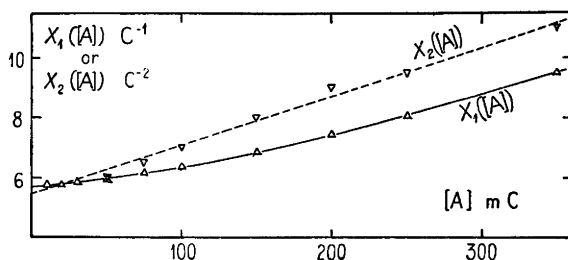


Fig. 6.  $X_1([A])$  and  $X_2([A])$  which give the complexity constants.

not very reliable, as was mentioned above. The straight lines have the intercept on the  $C_A$ -axis =  $[A]$  and the slope =  $\bar{n}$ , Table 4. The points are further plotted in Fig. 4. It is immediately seen from the complex formation curve so obtained, that the points from the two  $\lambda$  used are situated entirely on the same curve, and thus give the same complexity constants. The criterion of Güntelberg thus also speaks in favour of a mononuclear complex formation.

We may therefore consider the complex formation curve determined as substantial and calculate the constants from it. So the function  $\bar{n}/[A] = f([A])$  is formed, Fig. 5, and hence the function  $X([A])$  is obtained by integration according to (5 a) of II. From  $X([A])$ ,  $X_1([A])$  and  $X_2([A])$  are formed according to (7) of II (Table 5) and plotted in Fig. 6. From  $X_1([A])$  we obtain  $\beta_1 = 5.7 \pm 0.3$  and from  $X_2([A])$ , which is a straight line,  $\beta_2 = 5.5 \pm 1$  and  $\beta_3 = 15 \pm 5$ , with indicated accidental errors.

With these constants,  $\bar{n}$  is calculated at some round  $[A]$  according to (2) of II (Table 5) and introduced in Fig. 4 as a fulldrawn curve. It is seen to fit the experimental points very well. The composition of the system at the same  $[A]$  is calculated according to (8) of II and also given in Table 5.

The complexity of the uranyl thiocyanate system is thus very weak. This is perhaps a little unexpected as the extinction curve of  $\text{UO}_2^{2+}$  changes in such a substantial manner by addition of thiocyanate. It is now evident that this remarkable change must be due to an unusually great difference of  $\epsilon$  between  $\text{UO}_2^{2+}$  and its thiocyanate complexes. Even small quantities of these complexes therefore cause great changes in  $\epsilon_M$ . The result urges to the greatest caution at qualitative estimations of the stability of complexes on the basis of extinctionmetric measurements.

#### SUMMARY

The complexity of the uranyl thiocyanate system in aqueous solution is extinctionmetrically investigated. The measurements are performed at 20° C and at the ionic strength  $I = 1$ , which is brought about by  $\text{NaClO}_4$  and 100

mC  $\text{HClO}_4$ . The latter presses the hydrolysis of  $\text{UO}_2^{2+}$  back to a value which may be neglected.

According to both the criteria applied, no polynuclear complexes seem to exist in this system. The first three complexes of the mononuclear series are proved. Their constants, defined by (6) of I, are at the existing conditions

$$\beta_1 = 5.7 \qquad \beta_2 = 5.5 \qquad \beta_3 = 15$$

My thanks are due to *Försvarets Forskningsanstalt* (FOA), Stockholm, for a financial support.

#### REFERENCES

1. Ahrland, S. *Acta Chem. Scand.* 3 (1949) 783 (referred to as II).
2. Fronæus, S. *Diss.* Lund (1948).
3. Güntelberg, E. *Diss.* Copenhagen (1938).
4. Ahrland, S. *Acta Chem. Scand.* 3 (1949) 374 (referred to as I).
5. Ostwald, W. *J. prakt. Chem.* [2] 32 (1885) 305.
6. Gorman, M., and Connell, J. *J. Am. Chem. Soc.* 69 (1947) 2063.
7. Mann, C. *Z. anal. Chem.* 28 (1889) 668 (from Treadwell, F. P. *Kurzes Lehrbuch der analytischen Chemie*. 13th ed., Wien and Leipzig (1923) p. 321.
8. v. Kiss, A., and Csokan, P. *Z. physik. Chem. A* 186 (1940) 239.
9. Fromherz, H., and Menschick, W. *Z. physik. Chem. B* 7 (1930) 439.
10. Gmelins *Handbuch der anorganischen Chemie*. 8th ed. 55 (1936) 257.

Received June 9, 1949.